Macromolecules
ARTICLE

Macromolecules **2009**, *42*, 8751–8762 **8751**
DOI: 10.1021/ma901659q

Synthesis of Early Transition Metal Bisphenolate Complexes and Their Use as Olefin Polymerization Catalysts

Suzanne R. Golisz and John E. Bercaw*

Arnold and Mabel Beckman Laboratories of Chemical Synthesis, California Institute of Technology, Pasadena, California 91125

Received July 28, 2009; Revised Manuscript Received October 15, 2009

ABSTRACT: Bisphenolate ligands with pyridine- and benzene-diyl linkers have been synthesized and metalated with group 4 and 5 transition metals. The solid-state structures of some of the group 4 complexes have been solved. The titanium, zirconium, hafnium, and vanadium complexes were tested for propylene polymerization and ethylene/1-octene copolymerization activities with methylaluminoxane as cocatalyst. The vanadium(III) precatalyst is the most active for propylene polymerization and shows the highest 1-octene incorporation for ethylene/1-octene copolymerization. The zirconium(IV) precatalyst was the most active for propylene polymerization of the group 4 precatalysts. Titanium(IV) and zirconium(IV) precatalysts with pyridine-diyl linkers provided mixtures of isotactic and atactic polypropylene while titanium(IV) precatalysts with benzene-diyl linkers gave atactic polypropylene only. The hafnium(IV) precatalyst with a pyridine-diyl linker generated moderately isotactic polypropylene.

Introduction

Polymers are ubiquitous materials with applications in household products, biomedicine, and transportation. The polymerizations of ethylene, propylene, and styrene with Ziegler−Natta catalysts represent important processes that have grown to a worldwide production exceeding 100 billion pounds per year.[1] Understanding the influence of catalyst structure on polymer composition and microstructure allows for the development of polymer architectures with various applications.[2−7] Single-site catalysts are amenable to these types of studies such that an enormous number of metallocene and nonmetallocene catalysts have been synthesized in the past 30 years.[2,6] Metallocene catalysts are well understood with respect to the relationship between catalyst symmetry and polymer microstructure (Figure 1).[4] However, nonmetallocene catalysts represent a less understood sector of polymerization catalysts with respect to catalyst symmetry−polymer microstructure relationships.[3,5]

Given the promising ability of non-metallocene catalysts to control polymer tacticity, we found it desirable to synthesize a new type of ligand for detailed study. This non-metallocene ligand framework features a bidentate or tridentate moiety with two anionic donors positioned around a central atom or donor connected at the *ortho* position via semirigid sp^2-sp^2 linkages (see Figure 1). We and others have begun to explore the polymerization activities and selectivities of group 4 complexes with these ligands.[8−12] Herein we disclose the synthesis of bisphenolate pyridine- and benzene-diyl linked ligands. Group 4 and 5 complexes supported by these ligands have been prepared, and their utility as polymerization catalysts has been examined, including their influence on molecular weight and ability to control polymer tacticity.

Results and Discussion

Ligand Synthesis. The ligands (**1-H_2**, **2-H_2**, **3-H_2**, and **4-H_2**) were synthesized with overall yields ranging from 20% to 60% (Scheme 1). The acid-promoted alkylation of *p*-cresol with 1-adamantanol was previously reported.[13] Both o*rtho*-bromination and deprotonation with sodium hydride followed by protection with chloromethyl methyl ether (MOM-Cl) occur in high yield. In the case of the adamantyl-substituted species, the deprotonation/protection reaction produced an unidentifiable byproduct which was removed by Kugelröhr distillation. The coupling reaction of the protected bromophenol with either 2,6-dibromopyridine or 1,3-dibromobenzene was achieved through lithium−halogen exchange followed by transmetalation using $ZnCl_2$ and palladium-catalyzed Negishi cross-coupling.[14] The protecting group (MOM) was removed by treatment with acidic methanol at 65 °C. Simple filtration of the methanol solution afforded the adamantyl-substituted ligands (**1-H_2** and **3-H_2**). The *tert*-butyl-substituted ligands (**2-H_2** and **4-H_2**) were obtained by solvent removal. The identity of the ligands was confirmed by ^{1}H NMR spectroscopy, ^{13}C NMR spectroscopy, and HRMS.

Preparation of Metal Complexes. The ligands (or their dianions) were treated with the appropriate early transition metal precursors ($TiCl_4(THF)_2$, $Ti(OCH(CH_3)_2)_4$, $Ti(CH_2C_6H_5)_4$, $Zr(CH_2C_6H_5)_4$, $Hf(CH_2C_6H_5)_4$, or $VCl_3(THF)_3$ where $OCH(CH_3)_2$ = O^{i}Pr and $CH_2C_6H_5$ = Bn) to give the desired products (Schemes 2 and 3). The salt metathesis reaction with $TiCl_4(THF)_2$ or $VCl_3(THF)_3$ involved initial deprotonation of the ligand with potassium benzyl. The KCl byproduct was removed by filtration. Repeated attempts using the salt metathesis routes with $ZrCl_4(THF)_2$ or $HfCl_4(THF)_2$ proved unsuccessful because substantial amounts of the bis-ligated species formed under a variety of conditions. (The bis-ligated species was identified by ^{1}H NMR spectroscopy data from independent synthesis using an excess of ligand with $ZrBn_4$.[8]) The alcohol elimination reaction with $Ti(O^iPr)_4$ lead to the desired product only when heated at 80 °C overnight. Alkane elimination reactions were successfully employed with the tetrabenzyl derivatives of the entire group 4 series. All metal complexes were characterized by

*Corresponding author. E-mail: bercaw@caltech.edu.

Published on Web 10/29/2009

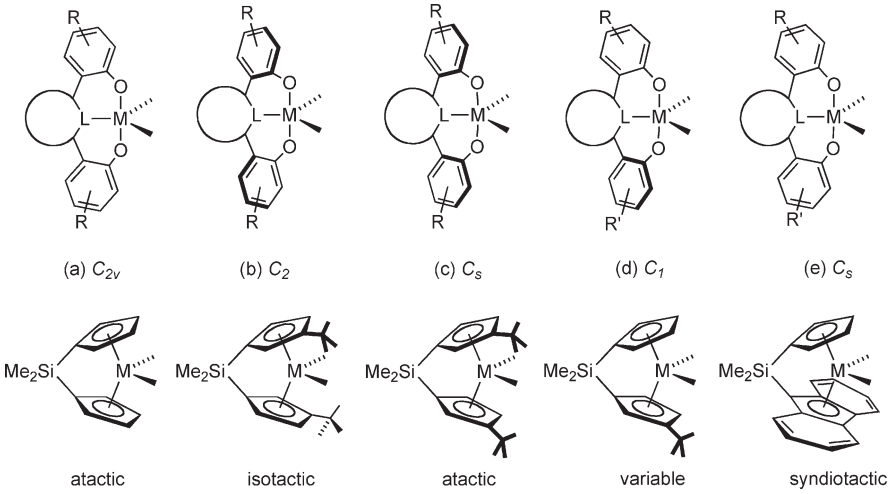

Figure 1. Relationship between catalyst geometry and anticipated polymer microstructure where R = alkyl, linker = pyridine-diyl or benzene-diyl, and L = N (neutral) or C (neutral or anionic).

NMR spectroscopy with the exception of the paramagnetic vanadium complex (vide infra). Further confirmation was obtained through elemental analysis, and in some cases, X-ray quality crystals were grown.

As shown previously, these complexes display different solution-state geometries (C_{2v}, C_s, C_2, or C_1) that may, in principle, be assigned by ^{1}H NMR spectroscopy through analysis of the benzyl [CH_2] protons: (1) C_{2v} geometry is expected to lead to a singlet, (2) C_s geometry should give two singlets, (3) C_2 geometry makes the [CH_2] protons diastereotopic, which should lead to two doublets, and (4) C_1 geometry would make all four benzylic protons different, appearing as four doublets.[8] All complexes with pyridine-diyl linkers (**1-TiBn$_2$, 2-TiBn$_2$, 1-ZrBn$_2$,** and **1-HfBn$_2$**) featured one singlet between 3.1 and 4.1 ppm integrating as four benzyl protons, implying either a C_{2v} geometry or dynamic equilibration of methylene hydrogens for a lower symmetry structure to give a singlet on the NMR time scale. The complexes with benzene-diyl linkers (**3-TiBn$_2$** and **4-TiBn$_2$**) showed two singlets between 1.9 and 3.7 ppm with each signal attributed to two benzyl protons, indicating (time-averaged) C_s geometry. These geometry assignments were corroborated by X-ray crystallography data.

The orange/brown solid of **1-VCl(THF)$_2$** was paramagnetic and showed very broad peaks in the ^{1}H NMR spectrum. The solution magnetic susceptibility was determined using the Evans method to give a $\mu_{\text{eff}} = 2.90(2)\ \mu_B$.[15] This matches the predicted value (μ_{eff}(spin only) = 2.82) for two unpaired electrons in trivalent vanadium complexes. The presence of two coordinated THF molecules was confirmed by elemental analysis.

X-ray Crystal Structures. Colorless single crystals suitable for X-ray diffraction of **1-Ti(O^{i}Pr)$_2$** were serendipitously obtained from a benzene-d_6 solution in a J. Young NMR tube (Figure 2). The complex shows C_2 symmetry around the metal center with pseudo-trigonal-bipyramidal geometry (crystal and refinement data can be found in Table 1). The bond lengths of Ti1−O1 and Ti1−O2 (the oxygens of the phenolate moieties) are essentially identical to each other at 1.92 Å. The Ti1−O3 and Ti1−O4 bonds (where the oxygens are from the alkoxides) are also identical at 1.75 Å. The twist angle (defined as the angle between the Ti−O$_{\text{phenolate}}$ bond and the N−C$_{ortho}$ bond) of **1-Ti(O^{i}Pr)$_2$** is 36°.

Single crystals of **1-ZrBn$_2$(Et$_2$O)** were obtained by cooling a diethyl ether (Et$_2$O) solution of **1-ZrBn$_2$** to −35 °C (Figure 3). The complex adopts a pseudo-octahedral geometry at zirconium due to the coordinated diethyl ether with C_s symmetry (crystal and refinement data can be found in Table 1). The pyridine ring is canted ∼42° from either of the planes of the phenolate rings, similar to previous observations for tantalum and zirconium complexes with closely related ligands.[8,16,17] This canting allows one of the benzyl groups (C40, C41) to sit in the space vacated by the pyridine. The presence of a coordinated diethyl ether appeared to be an effect of crystallization only. When the synthesis of **1-ZrBn$_2$** was carried out in diethyl ether followed by removal of the solvent to give a solid, which was dissolved in benzene-d_6, no coordinated diethyl ether was observed in the ^{1}H NMR.

Dark red crystals of **4-TiBn$_2$** were obtained by cooling a concentrated solution in petroleum ether to −35 °C overnight (Figure 4). The geometry about titanium is pseudo-tetrahedral as the closest carbon from the benzene-diyl linker (C18) is greater than 2.9 Å from Ti1 (crystal and refinement data can be found in Table 1). The ligand is arranged in a nearly C_s fashion, while the overall symmetry of the complex is C_1 due to the asymmetry in the placement of the benzyl groups. This geometry creates a large void on the backside of the complex (below C36 and behind C18). The plane of the benzene-diyl linker is canted further (∼48°) from the plane of the phenolates than in the case of **1-ZrBn$_2$(Et$_2$O)**. This is mostly likely a result of the fact that there is no bond between Ti1 and C18 (vide supra). The observation of separate singlets for the two benzyl methylene protons in the ^{1}H NMR spectrum at room temperature (vide supra) indicates that interconversion of benzyls via pivoting of the benzene-diyl about the *ipso* C$_{\text{benzene-diyl}}$−C$_{\text{phenolate}}$ linkages has a substantial barrier.

Propylene Polymerization with Ti, Zr, Hf, and V Precatalysts. Propylene polymerizations have been performed in the presence of methylaluminoxane (MAO) as cocatalyst for all group 4 and 5 precatalysts herein synthesized. The sole exception was **1-Ti(O^{i}Pr)$_2$,** which could not be activated by MAO, possibly due to the relative strength of Ti−O$_{\text{isopropoxide}}$ vs Al−O bonds. All polymerizations were performed at 0 °C for 30 min[18] in 2 mL of toluene with a minimum of 1000 equiv of MAO and essentially liquid propylene, [C$_3$H$_6$] = 12 M.[19] The effect of precatalyst on activity, molecular weight, and tacticity has been investigated (Table 2). The polypropylenes (PP) were analyzed by gel permeation chromatography (GPC) and ^{13}C NMR.

Scheme 1

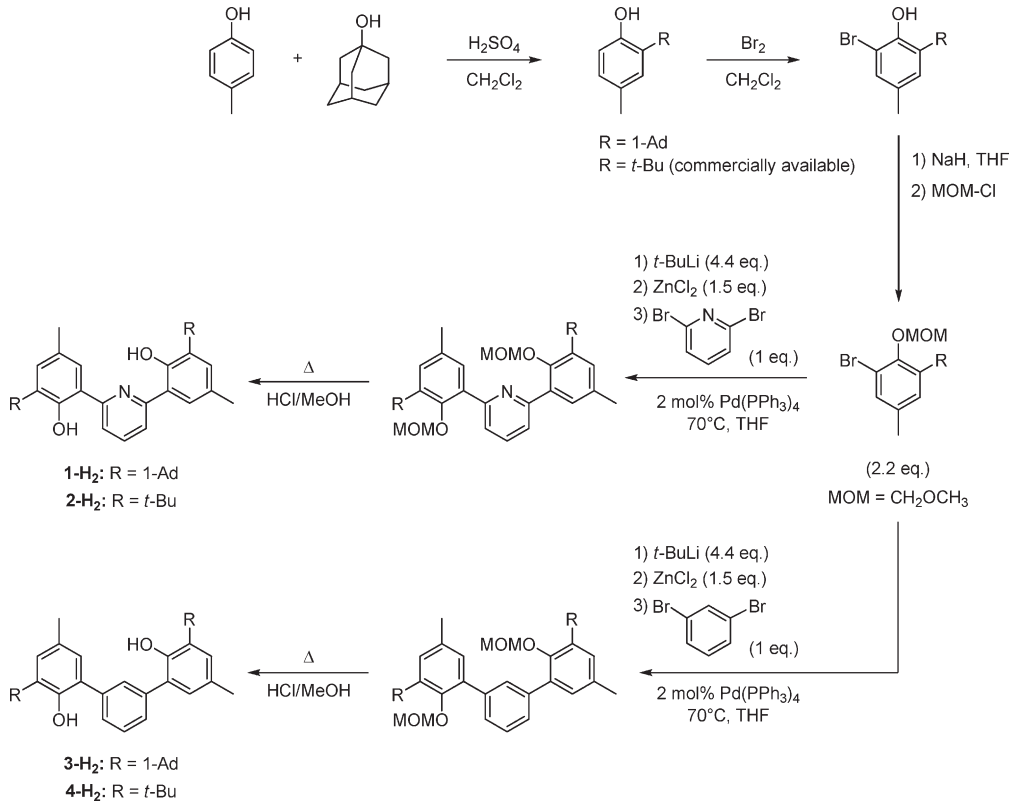

Scheme 2

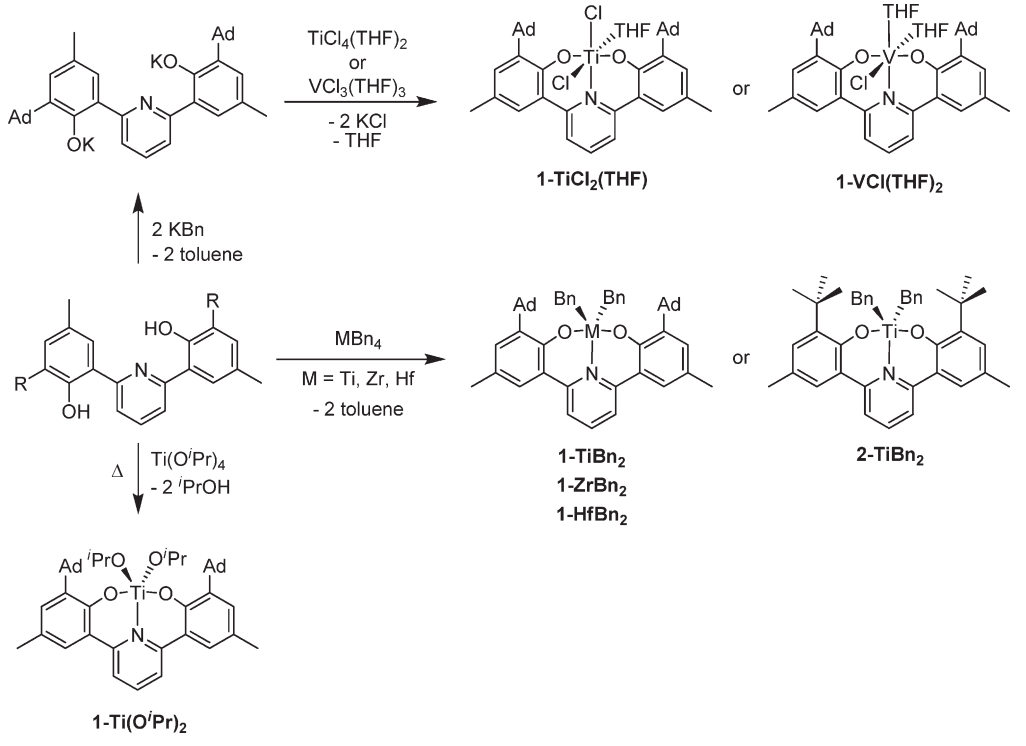

The vanadium precatalyst is the most active. Molecular weight analysis of the resulting PP shows narrow polydispersity with a number-average molecular weight greater than 500 000 g/mol. The ^{13}C NMR spectrum shows slight syndiotactic enrichment with a large amount of the 2,1-erythro regioerror common to many vanadium polymerization catalysts (Figure 5).[20] This polymer is rather insoluble with blue/green particles (residual vanadium) dispersed amid the white polymeric mass. The insolubility is possibly due, in part, to the high molecular weight. The PDI of ~2 indicates only one active catalytic species. It is difficult to conclusively determine the active species because vanadium can access a

Scheme 3

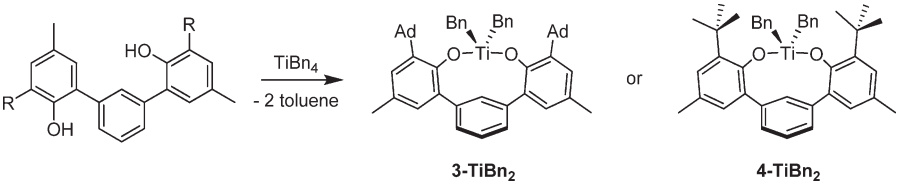

3-TiBn$_2$ **4-TiBn$_2$**

variety of oxidation states. Current theories suggest that V(II), V(III), V(IV), and V(V) may all be catalytically active oxidation states in olefin polymerization.[21] A few vanadium-(III) precatalysts have been examined for their activity for olefin polymerization; while most of these precatalysts are active for ethylene polymerization or oligomerization,[22] those same precatalysts show little or no activity for propylene.[23] A tris(2-methyl-1,3-butanedionato)vanadium precatalyst showed activity of 470 kg PP mol cat.$^{-1}$ h^{-1} at 0 °C with an [Al]/[V] ratio of 400 where the cocatalyst was Al-$(C_2H_5)_2$Cl.[24]

Comparing the linking groups, there is a marked increase in activity going from the pyridine-diyl linker to the benzene-diyl linker (compare **1-TiBn$_2$** to **3-TiBn$_2$**); however, both of these linking groups are less active than the furan-diyl or thiophene-diyl linking groups which generate propylene oligomers.[8] A zirconium dibenzyl precatalyst featuring a tetradentate [ONNO]-type ligand was found to be 2 orders of magnitude more active for propylene polymerization (11 500 kg PP mol^{-1} h^{-1} at 50 °C) than **1-ZrBn$_2$**.[25] The more interesting observation is the difference in molecular weight depending on the linking group. For all group 4 precatalysts with pyridine-diyl linked bisphenolate ligands, the molecular weight distribution is very broad and in some cases bimodal, indicating the presence of more than one catalytically active species. On the contrary, the precatalysts with benzene-diyl linked bisphenolate ligands feature narrow PDI (~2), suggesting that only one species is responsible for polymer formation.

Most of the PPs generated were quite insoluble and required heating above 120 °C in $C_2D_2Cl_4$ or $C_6D_4Cl_2$ to reach the concentration necessary for acceptable ^{13}C NMR data. ^{13}C NMR for PP generated from **1-TiCl$_2$(THF)** is typical for group 4 precatalysts and is shown in Figure 6. Group 4 precatalysts generate mostly regioregular PP with minimal amounts of the 2,1-erythro error.[26] Further analysis of the methyl region revealed an interesting motif where the *mmmm* pentad was enhanced relative to the other pentads. The other pentads resembled statistically atactic polypropylene (aPP). This motif appeared in the PP from titanium and zirconium precatalysts with pyridine-diyl linkers (Figure 7). On the other hand, the benzene-diyl linked precatalysts generated only aPP, and the hafnium precatalyst produced moderately (*mmmm* = 40%) isotactic polypropylene (iPP).

Fractionation of Polypropylene Produced by 1-TiCl$_2$(THF). To determine whether the motif observed with **1-TiCl$_2$(THF)**, **1-TiBn$_2$**, **2-TiBn$_2$**, and **1-ZrBn$_2$** (Figure 7a−d) was a new type of polymer or a result of multiple polymers, a PP sample produced with **1-TiCl$_2$(THF)** was extracted from a paper thimble by a series of refluxing solvents (diethyl ether, hexanes, and heptanes) such that the polymer was separated on the basis of difference in tacticity.[27] About half of the polymer (by weight) dissolved in diethyl ether (Table 3). Very little of the polymer was soluble in either hexanes or heptanes. The other half of the polymer (by weight) was insoluble in all solvents tested. ^{13}C NMR was obtained for both major fractions (Figure 8). The diethyl ether soluble fraction is essentially low molecular weight aPP. The insoluble fraction had a significant amount of residual aluminum, most likely from inefficient removal of the MAO (this was confirmed by elemental analysis: C, 2.44; H, 3.22; Al, 32.7) which made initial attempts to obtain ^{13}C NMR data quite difficult. Prolonged stirring in acidified methanol removed enough aluminum such that a very dilute sample of the polymer component remained. ^{13}C NMR analysis of a dilute sample indicated iPP; however, due to the poor signal-to-noise ratio in that spectrum, triad analysis for mechanism of stereocontrol was not reliable.[28−31] The fractionation experiment confirmed that group 4 pyridine-diyl linked precatalysts[32] generated two different types of polymer (iPP and aPP), most likely from two catalytically active species.

Stoichiometric Activation. In most cases, stoichiometric activation of the dibenzyl complexes with $[C_6H_5NH(CH_3)_2][B(C_6F_5)_4]$ or $[(C_6H_5)_3C][B(C_6F_5)_4]$ in the presence of propylene gave no polymer. For one experiment in which tri(isobutyl)aluminum (TIBA, 50 equiv) was added as an air and moisture scavenger, a small amount of polymer was obtained (10 mg of polymer for 5 mg of precatalyst). Because of the low activity, this polymer was not analyzed.

Treating the benzene-diyl linked precatalyst **4-TiBn$_2$** with less than 1 equiv of activator (~13 mol %) gave toluene and the benzene-diyl metalated dimeric species **[4-TiBn]$_2$** with the formula $\{Ti(CH_2C_6H_5)[(OC_6H_2\text{-}2\text{-}C(CH_3)_3\text{-}4\text{-}CH_3)C_6H_3\text{-}(2\text{-}C(CH_3)_3\text{-}4\text{-}CH_3C_6H_2\text{-}\mu^2\text{-}O]\}_2$ where a phenolate from one titanium bridges to the other titanium (this complex has been fully characterized and will be described in a forthcoming article; see Figure S1 for a schematic).[33] We considered the possibility that this dimeric complex, which, surprisingly, contains a C_2-symmetric cyclometalated tridentate ligand, could act as an olefin polymerization catalyst without the addition of cocatalyst (MAO). To test this idea, the dimeric species **[4-TiBn]$_2$** was introduced to an atmosphere of ethylene in a J. Young NMR tube and, in a separate experiment, was subjected to the standard propylene polymerization conditions. Neither experiment showed polymer production. It was therefore concluded that the C_2-symmetric species was not active for olefin polymerization. By extension, the only benzene-diyl linked catalyst which is active for olefin polymerization is the C_s-symmetric Ti−benzyl cationic species derived from **4-TiBn$_2$** (Scheme 4).

The Role of Aluminum. It was previously observed that the ratio of low molecular weight PP to high molecular weight PP and thus aPP to iPP (produced from **2′-ZrBn$_2$** where the *para* methyl group has been replaced by a *tert*-butyl group) changed with the number of equivalents of MAO, where an increased amount of MAO favored the low molecular weight aPP.[8] This implied that the MAO may be interacting in such a way to influence the relative concentrations of the active catalytic species. Possibilities include transmetalation to generate an aluminum catalyst and modification of the ligand by aluminum. To test the first hypothesis, control reactions were performed to show that bisphenolate ligated aluminum methyl species were not competent catalysts for propylene polymerization.[34] Regarding the second possibility, aluminum has been shown to reduce C=N bonds to the

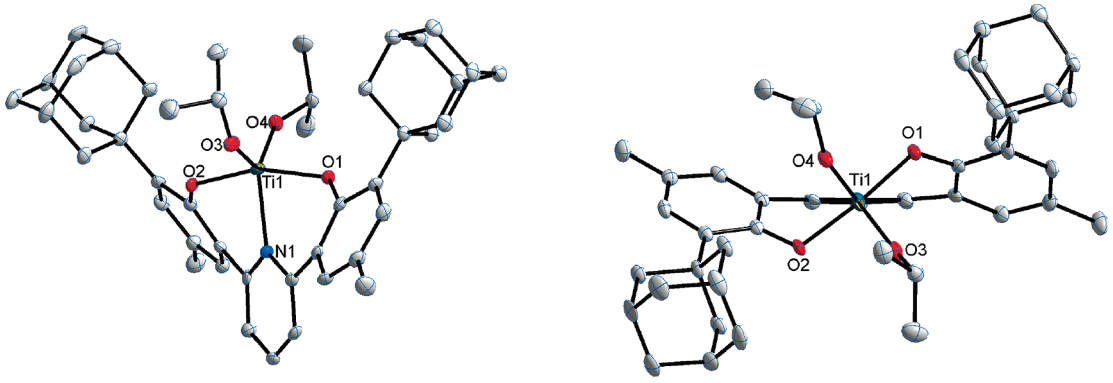

Figure 2. Solid-state structure of **1-Ti(O^{i}Pr)$_2$**. The top view is shown on the right, looking down the Ti1−N1 bond. Hydrogens have been omitted for clarity. Selected bond lengths (Å) and angles (deg): Ti1−N1 2.169(2), Ti1−O1 1.92(19), Ti1−O2 1.92(18), Ti1−O3 1.758(2), Ti1−O4 1.75(18), O1−Ti1−O2 159.79(8), N1−Ti1−O1 79.53(8), N1−Ti1−O2 80.84(8).

Table 1. Crystal and Refinement Data for 1-Ti(O^{i}Pr)$_2$, 1-ZrBn$_2$(Et$_2$O), and 4-TiBn$_2$

	1-Ti(O^{i}Pr)$_2$	1-ZrBn$_2$(Et$_2$O)	4-TiBn$_2$
empirical formula	$C_{45}H_{57}NO_4Ti \cdot 2.5(C_6H_6)$	$C_{57}H_{67}NO_3Zr \cdot C_4H_{10}O$	$C_{42}H_{46}O_2Ti$
formula weight	919.09	979.46	630.69
crystal size (mm^3)	0.33 × 0.26 × 0.05	0.27 × 0.21 × 0.07	0.37 × 0.18 × 0.12
temperature (K)	100(2)	100(2)	100(2)
a (Å)	13.206(3)	9.971(5)	11.811(6)
b (Å)	13.234(3)	11.280(6)	12.473(7)
c (Å)	15.814(3)	23.361(13)	13.659(7)
α (deg)	80.36(4)	97.9(10)	100.57(3)
β (deg)	67.61(4)	101.8(10)	100.81(3)
γ (deg)	74.12(4)	95.2(10)	102.04(3)
volume (Å^3)	2451.7(8)	2528.6(2)	1880.5(17)
Z	2	2	2
crystal system	triclinic	triclinic	triclinic
space group	$P\bar{1}$ (#2)	$P\bar{1}$ (#2)	$P\bar{1}$ (#2)
d_{calc} (mg/m^3)	1.245	1.286	1.114
θ range (deg)	1.71−28.36	1.80−33.76	1.81−37.31
μ (mm^{-1})	0.224	0.266	0.259
abs correction	none	none	none
GOF	1.17	1.15	2.28
R_1,[a] wR_2[b] [$I > 2\sigma(I)$]	0.056, 0.099	0.044, 0.073	0.050, 0.088

[a] $R_1 = \sum||F_o| - |F_c||/\sum|F_o|$. [b] $wR_2 = [\sum[w(F_o^2 - F_c^2)^2]/\sum[w(F_o^2)^2]]^{1/2}$.

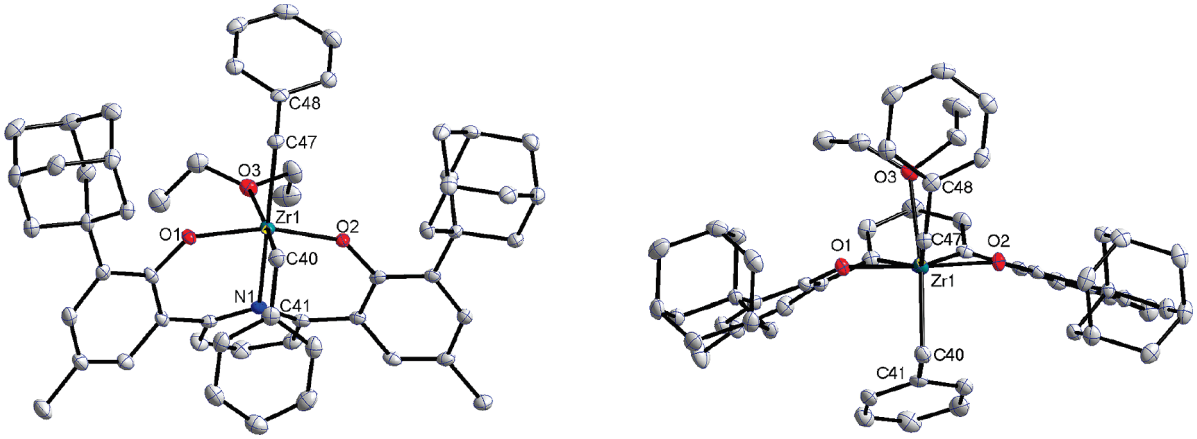

Figure 3. Solid-state structure of **1-ZrBn$_2$(Et$_2$O)**. The top view is shown on the right, looking down the Zr1−N1 bond. Hydrogens have been omitted for clarity. Selected bond lengths (Å) and angles (deg): Zr1−N1 2.47(13), Zr1−O1 1.98(11), Zr1−O2 1.98(12), Zr1−C40 2.29(16), Zr1−C47 2.32(16), Zr1−O3 2.39(11), O1−Zr1−O2 158.53(4), C48−C47−Zr1 120.6(11), C41−C40−Zr1 98.3(10).

amide functionalities and phenoxy-imine ligands to phenoxy-amines.[35−37] Additional experiments were performed on the bisphenolate system to determine whether MAO reacted irreversibly with the ligand.[38] Neither free pyridine-diyl linked ligand nor the complementary group 4 dibenzyl complex showed ligand modification with MAO at room temperature or upon heating.

It has become clear that group 4 pyridine-diyl linked precatalysts generate both low molecular weight aPP and high molecular weight iPP, benzene-diyl linked precatalysts generate only low molecular weight aPP from a C_s-symmetric active species, and bisphenolate ligated aluminum species are not competent olefin polymerization catalysts. Drawing from experience with metallocenes where the

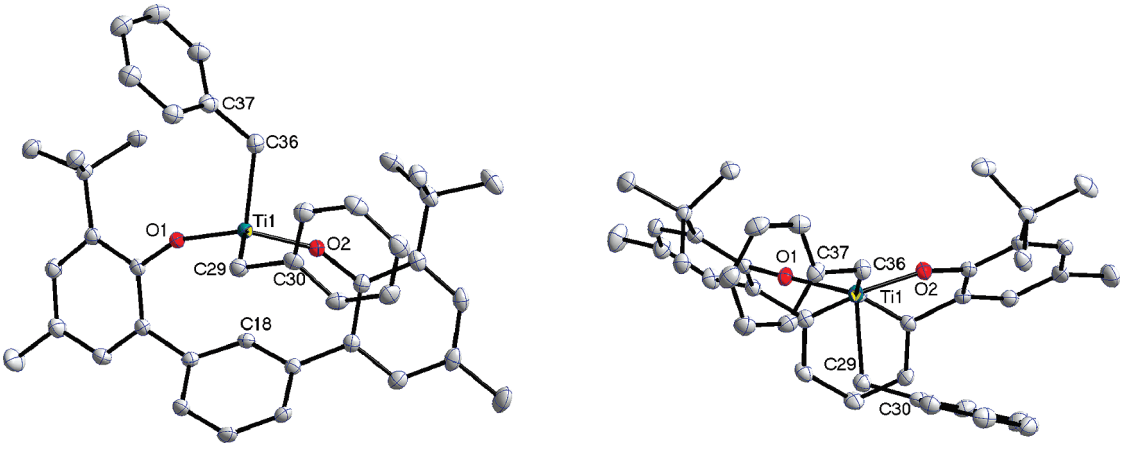

Figure 4. Solid-state structure of **4-TiBn$_2$**. The top view is shown on the right, looking down the Ti1−C18 vector. Hydrogens have been omitted for clarity. Selected bond lengths (Å) and angles (deg): Ti1−O1 1.812(7), Ti1−O2 1.805(7), Ti1−C29 2.10(11), Ti1−C36 2.09(11), O1−Ti1−O2 129.27(3), C29−Ti1−C36 101.46(4), Ti1−C36−C37 125.80(7), Ti1−C29−C30 110.53(7).

Table 2. Propylene Polymerization Results[a]

catalyst	catalyst loading (mg)	MAO (equiv)	yield (mg)	activity[b]	M_w	M_n	PDI
1-VCl(THF)$_2$	4.0	3000	2040	803	1117000	578000	2.03
1-TiCl$_2$(THF)	4.0	1000	44	17	576000	125000	4.60
1-TiBn$_2$	3.9	1000	23	9	2432000/11000	754000/6810	3.22/1.62
2-TiBn$_2$	30.0	1000	90	4	2468000	77500	31.8
1-ZrBn$_2$	6.2	1000	635	212	3630000/2600	513000/630	7.08/4.26
1-HfBn$_2$[c]	5.0	1000	17	3			
3-TiBn$_2$	30.0	1000	1600	72	11500	5960	1.94
4-TiBn$_2$	30.0	1000	1200	41	7500	3660	2.06
1-Ti(O^{i}Pr)$_2$	not activated by MAO						

[a] Conditions: propylene (5 atm, ~30 mL), toluene (2 mL), 0 °C, 30 m. [b] Activity = kg PP mol cat.$^{-1}$ h^{-1}. [c] The omission of data indicated that an insufficient amount of material was available for analysis.

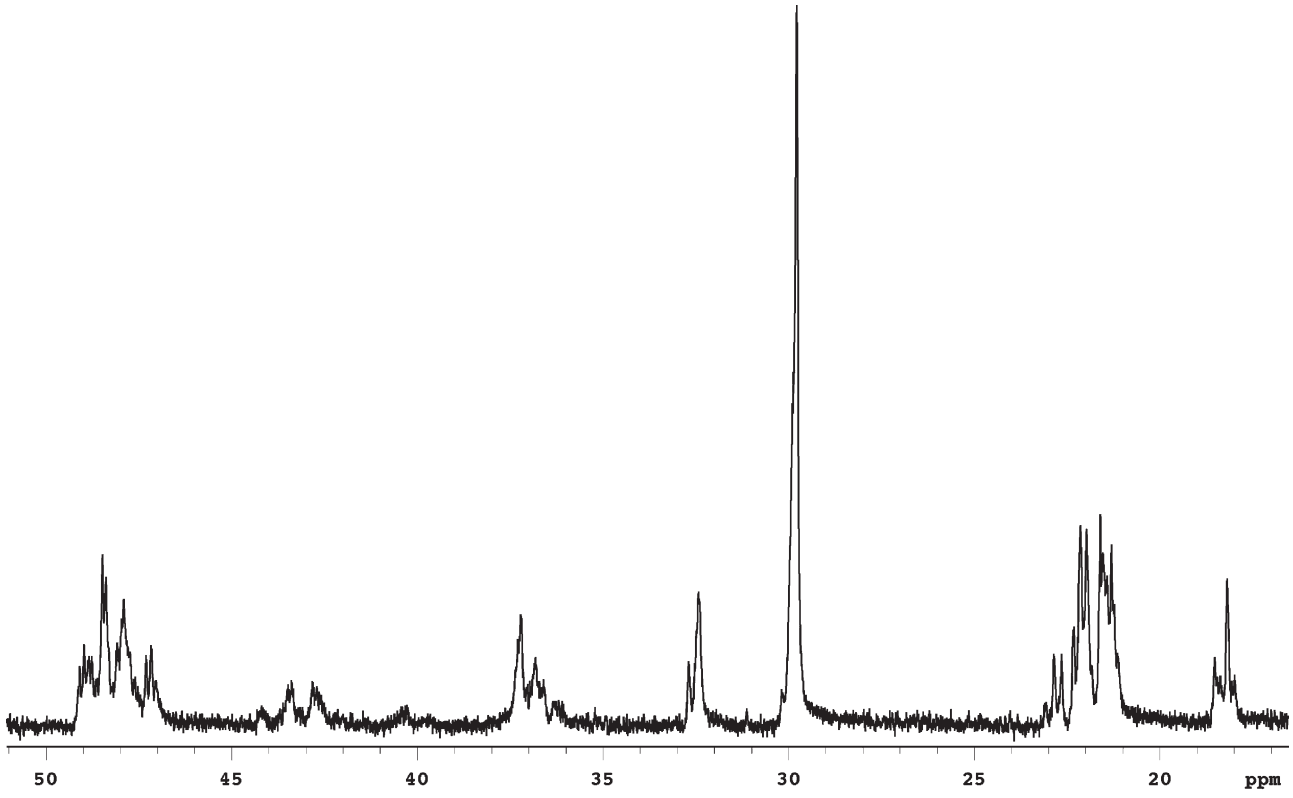

Figure 5. ^{13}C NMR spectrum of polypropylene produced with 1-VCl(THF)$_2$ in $C_2D_2Cl_4$.

geometry of the precatalyst dictates the polymer tacticity,[4] an analogous mechanism is possibly in operation here. The benzene-diyl linked precatalysts were shown to be C_s symmetric in the solution, solid, and (probably) active states;

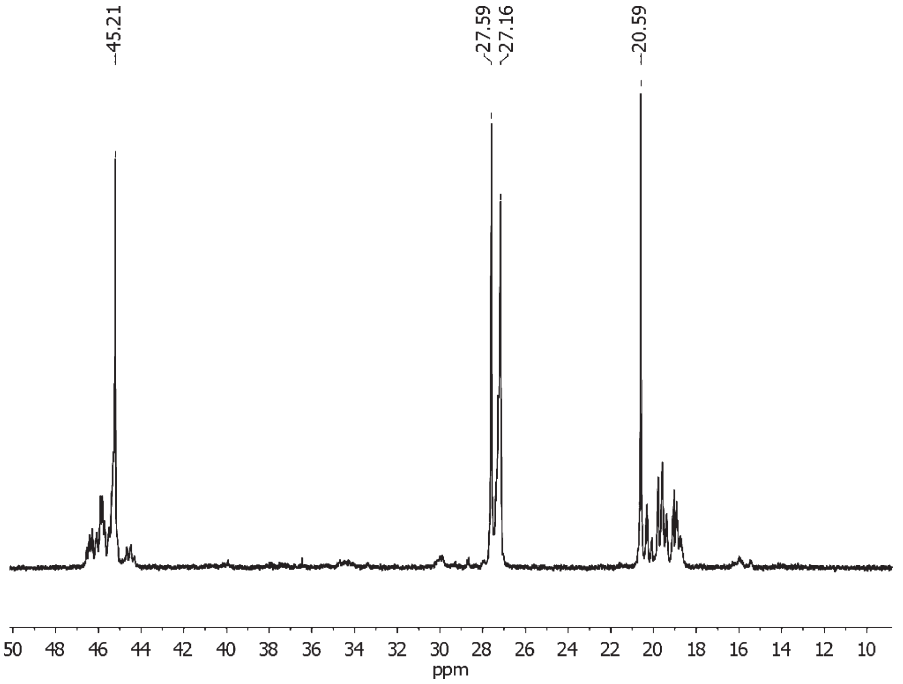

Figure 6. ^{13}C NMR spectrum of polypropylene produced with 1-$TiCl_2$(THF) in $C_6D_4Cl_2$.

C_s-symmetric catalysts are expected to give aPP as observed herein (Figure 1). The group 4 pyridine-diyl linked precatalysts exhibited a variety of different geometries; averaged C_{2v} symmetric in solution and either C_2 or C_s symmetric in the solid state depending on the coordination environment of the metal. We speculate that the group 4 pyridine-diyl linked precatalysts can access two different geometries in solution upon activation with MAO; a C_2-symmetric species which generates the iPP and a C_s-symmetric species which produces the aPP. Possibly, an interaction between the MAO and the nitrogen of the pyridine ring breaks the metal−nitrogen bond to give a C_s-symmetric species, while maintaining the M−N bond gives a C_2-symmetric species. Looking at the solid state structure of C_s-symmetric **4-TiBn$_2$** (Figure 4), there is a large vacancy under the benzyl group (C36 and C37) and behind the benzene-diyl linker. The canting of the pyridine ring in **1-ZrBn$_2$(Et$_2$O)** (Figure 5) sets up the nitrogen so that it points away from the metal and into that space. This void would be properly arranged for an aluminum species to interact with the nitrogen on the pyridine ring, thus generating a C_s-symmetric species.

Ethylene/1-Octene Copolymerization. The non-metallocene catalysts, **1-TiCl$_2$(THF), 1-ZrBn$_2$,** and **1-VCl(THF)$_2$**, were investigated to establish whether they are capable of producing ethylene/1-octene copolymers. In the presence of ethylene (1 atm) and 1-octene (ca. 50 vol %) in toluene with MAO as cocatalyst, all three precatalysts produced polymer (Table 4). The titanium catalyst had very low activity, and the resulting polymer could not be characterized. Both the zirconium and vanadium catalysts produced enough polymer for characterization.

The copolymers were analyzed by ^{13}C NMR (Figures S2 and S3) for the amount of comonomer incorporation (mol %).[39] The zirconium catalyst showed a large preference for ethylene over 1-octene. The vanadium catalyst was slightly more efficient at incorporating 1-octene into the growing polyethylene chain. Neither catalyst is capable of incorporating the amount of 1-octene necessary to produce an elastomer. Although no research group has disclosed the generation of ethylene/1-octene copolymers via vanadium precatalysts, a number of groups have reported ethylene/propylene copolymers.[24,40] There is also one known example of ethylene/1-hexene copolymerization where tridentate salicylaldiminato ligands on vanadium(III) in the presence of $Al(C_2H_5)_2Cl$ could incorporate up to 13 mol % 1-hexene.[41]

Conclusion

The bisphenolate ligands with both pyridine- and benzene-diyl linkers were metalated with group 4 and 5 metal precursors to give the desired complexes. These complexes were then found to be capable of olefin polymerization when activated with MAO. For the vanadium precatalyst, the activity for polypropylene was one of the highest of known V(III) olefin polymerization catalysts. Vanadium was also the most efficient at incorporating 1-octene into the ethylene/1-octene copolymer. In the case of group 4 pyridine-diyl linked bisphenolates, two different types of polymer were obtained: high molecular weight iPP and low molecular weight aPP. Conversely, benzene-diyl linked precatalysts generated only low molecular weight aPP. We speculate that the benzene-diyl linked precatalyst can access only a C_s-symmetric cationic catalyst species. The pyridine-diyl linked precatalyst can access two cationic catalyst species: a C_2-symmetric species which generates iPP and a C_s-symmetric species which produces aPP; the latter might arise from the coordination of aluminum (from MAO) to the pyridine.

Experimental Section

General Considerations. All air- and moisture-sensitive compounds were manipulated under argon or nitrogen using standard glovebox, Schlenk, and high-vacuum line techniques.[42] Argon and ethylene were purified and dried by passage through columns of MnO on vermiculite and activated 4 Å molecular sieves. Solvents were dried over sodium benzophenone ketyl or titanocene.[43] All organic chemicals, $ZrCl_4$, and VCl_3 were purchased and used as received from Aldrich. The metal precursors $TiCl_4$ and $Ti(O^iPr)_4$ were purchased from Strem and used as received. The $HfCl_4$ (99%) was purchased from Cerac and used as received. The activators methylaluminoxane (MAO), $[Ph_3C][B(C_6F_5)_4]$, and $[C_6H_5NH(CH_3)_2][B(C_6F_5)_4]$

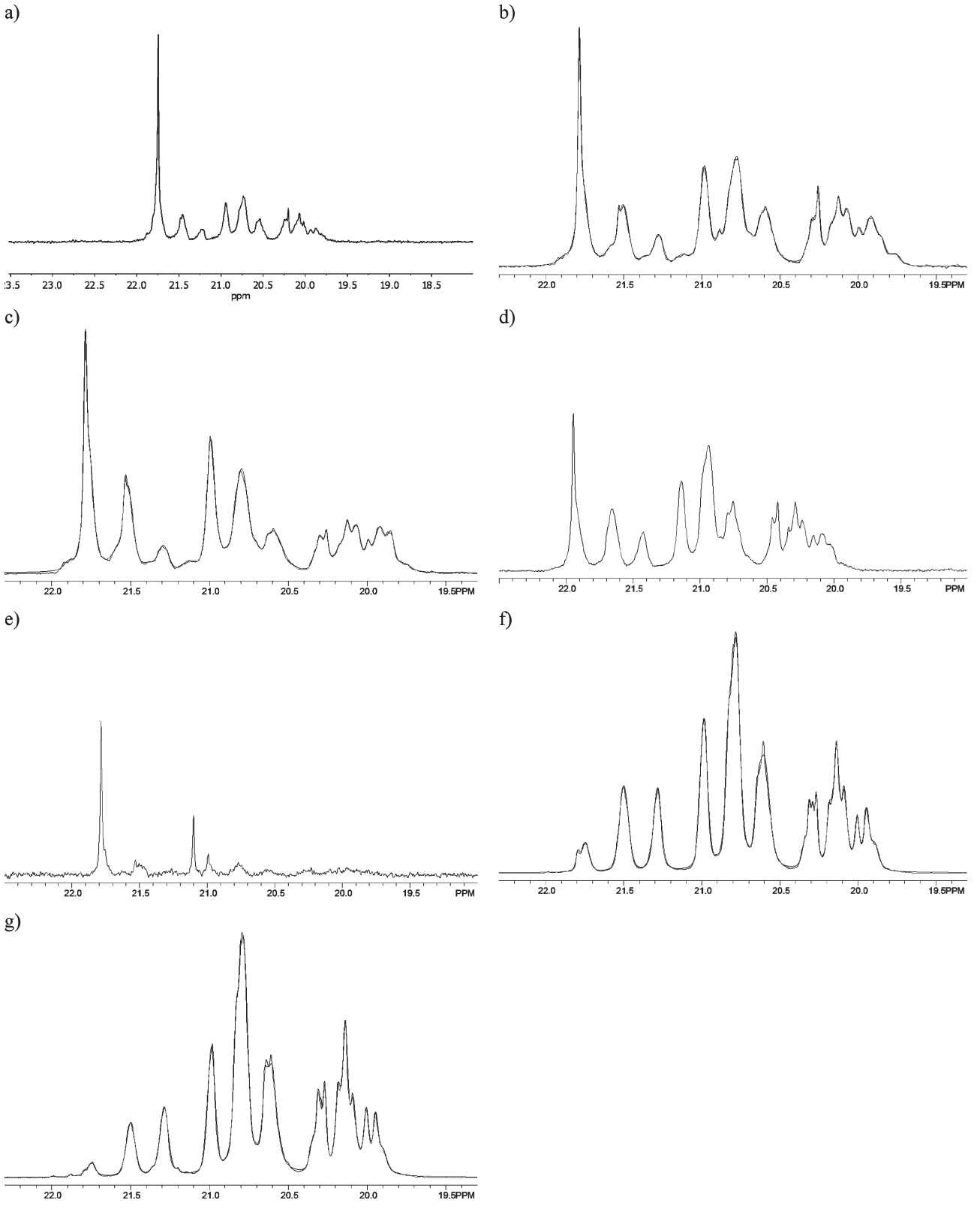

Figure 7. Expansion of the methyl region of the ^{13}C NMR (tetrachloroethane-d_2/*o*-dichlorobenzene-d_4 (1:4, v:v)) spectra of polypropylene produced with the following precatalysts: (a) **1-TiCl$_2$(THF)**, (b) **1-TiBn$_2$**, (c) **2-TiBn$_2$**, (d) **1-ZrBn$_2$**, (e) **1-HfBn$_2$**, (f) **3-TiBn$_2$**, (g) **4-TiBn$_2$**.

were purchased from Albemarle. The MAO was dried *in vacuo* at 150 °C overnight to remove free trimethylaluminum before use. Propylene was dried by passage through a Matheson 2110 drying system equipped with an OXISORB column. The concentration of propylene in toluene solutions was calculated according to literature data.[19] NMR spectra of ligands and precatalysts were recorded on a Varian Unity Inova 500 (499.852 MHz for ^1H) or Varian Mercury (300 MHz for ^1H) spectrometer. NMR solvents were purchased from Cambridge Isotope. Chemical shifts were reported using the residual solvent signal. Analysis by GC-MS was carried out on an HP 5890 Series II gas chromatograph connected to an HP 5972 mass

spectrometric detector. A 60 m × 0.32 μm internal diameter column was used which was coated with a 5 μm think 100% methylsiloxane film. High-resolution mass spectra (HRMS) were obtained from the California Institute of Technology Mass Spectrometry Facility. X-ray quality crystals were mounted on a glass fiber with Paratone-N oil. Data were collected on a Bruker KAPPA APEX II instrument. Structures were determined using direct methods or, in some cases, Patterson maps with standard Fourier techniques using the Bruker AXS software package. GPC data were generated on Symyx HT-GPC's using an IR4 detector, calibrated with narrow PS standards and adjusted for PP alpha and K's. 2-Adamantyl-4-methylphenol;[13] $TiCl_4(THF)_2$, $ZrCl_4(THF)_2$, $HfCl_4(THF)_2$, and $VCl_3(THF)_3$;[44] and tetrabenzyl complexes of group 4[45] were prepared according to literature procedures.

Table 3. Results of the Fractionation of Polypropylene Made from 1-$TiCl_2$(THF)

solvent	amount (g)	^{13}C NMR	M_w	M_n	PDI
initial	3.28	mixture			
diethyl ether soluble	1.50	aPP	21 000	9180	2.29
hexanes soluble	0.10				
heptanes soluble	0.10				
insoluble	1.58	iPP			

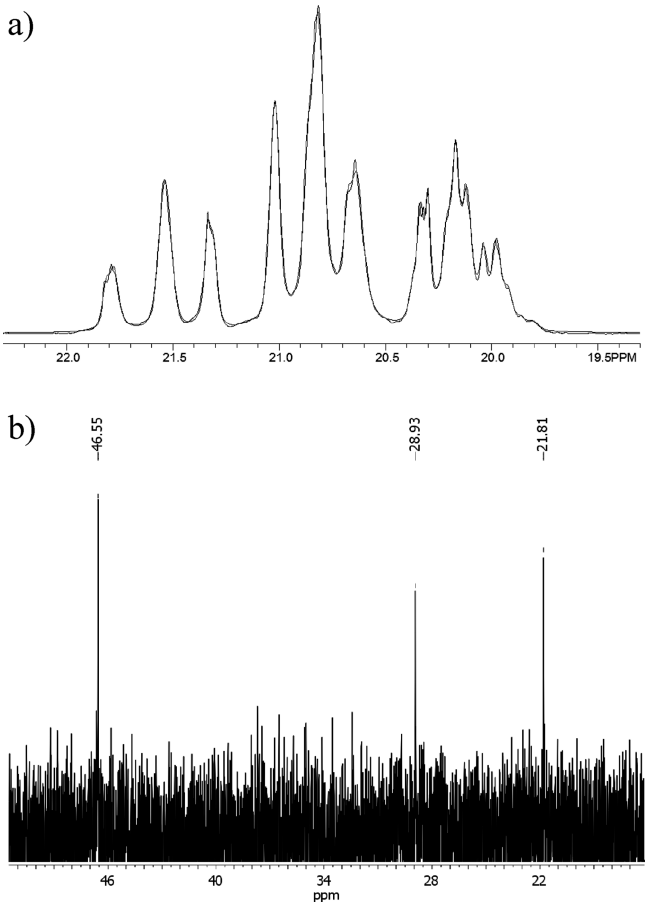

Figure 8. ^{13}C NMR spectra of the polypropylene produced by **1-$TiCl_2$(THF)** after fractionation: (a) an expansion of the methyl region for the diethyl ether soluble fraction and (b) insoluble fraction.

Synthesis of 2-Adamantyl-4-methyl-5-bromophenol. 2-Adamantyl-4-methylphenol (9.9 g, 40.9 mmol) was dissolved in CH_2Cl_2 (200 mL). Bromine (2.09 mL, 40.9 mmol) was added dropwise to the solution. After 20 min, GC-MS showed a single peak corresponding to the product. The crude mixture was washed with H_2O, dried over $MgSO_4$, filtered, and dried with a rotary evaporator to give a pale yellow solid: 10.6 g, 80%. ^{1}H NMR (300 MHz, $CDCl_3$): δ 1.78 (s, 6H, Ad), 2.11 (s, 9H, Ad), 2.26 (s, 3H, CH_3), 5.64 (s, 1H, O*H*), 6.96 (s, 1H, C_6H_2), 7.16 (s, 1H, C_6H_2).

Synthesis of 2-*tert*-Butyl-4-methyl-5-bromophenol. 2-*tert*-Butyl-4-methylphenol (16 g, 97.4 mmol) was dissolved in CH_2Cl_2 (200 mL). Bromine (5.0 mL, 97.4 mmol) was added dropwise to the solution. After 1.5 h, GC-MS showed a single peak corresponding to the product. The crude mixture was washed with H_2O, dried over $MgSO_4$, filtered, and dried with a rotary evaporator to give golden yellow oil: 22.7 g, 96%. ^{1}H NMR (500 MHz, $CDCl_3$): δ 1.40 (s, 9H, $C(CH_3)_3$), 2.27 (s, 3H, CH_3), 5.64 (s, 1H, O*H*), 7.02 (s, 1H, C_6H_2), 7.17 (s, 1H, C_6H_2). ^{13}C NMR (125 MHz, $CDCl_3$): δ 20.55, 29.37, 35.26, 111.87, 127.35, 129.59, 130.21, 137.17, 148.13. HRMS (FAB+) obsd (M + H)−H_2 241.0236; calcd for $C_{11}H_{14}BrO$, 241.0228.

Protection of 2-Adamantyl-4-methyl-5-bromophenol. Sodium hydride (574 mg, 23.9 mmol) was suspended in anhydrous THF (10 mL). 2-Adamantyl-4-methyl-5-bromophenol (6.4 g, 19.9 mmol) was dissolved in anhydrous THF (100 mL) and transferred by cannula onto the sodium hydride suspension. The mixture became blue in color, and hydrogen gas was evolved. After 30 min, chloromethyl methyl ether (1.7 mL, 21.9 mmol) was syringed into the reaction flask. The mixture was stirred for 14 h. The mixture was concentrated, extracted in H_2O, washed with diethyl ether (50 mL, 3×), dried over $MgSO_4$, filtered, and dried with a rotary evaporator. The crude product was purified by Kugelröh distillation to give a white solid: 5.2 g, 71%. ^{1}H NMR (300 MHz, $CDCl_3$): δ 1.78 (s, 6H, Ad), 2.11 (s, 9H, Ad), 2.28 (s, 3H, CH_3), 3.72 (s, 3H, CH_2OCH_3), 5.22 (s, 2H, CH_2OCH_3), 7.05 (s, 1H, C_6H_2), 7.24 (s, 1H, C_6H_2).

Table 4. Ethylene/1-Octene Copolymerization Data[a]

catalyst	yield (mg)	activity[b]	comonomer incorporation (mol %)
1-$TiCl_2$(THF)[c]	20	3	
1-$ZrBn_2$	1200	160	0.5
1-$VCl(THF)_2$	374	50	6.6

[a] Conditions: ethylene (1 atm), 1-octene (2 mL), toluene (2 mL), MAO (1000 equiv), rt. [b] Activity = kg poly mol cat.$^{-1}$ h^{-1}. [c] The omission of data indicated that an insufficient amount of material was available for analysis.

Scheme 4

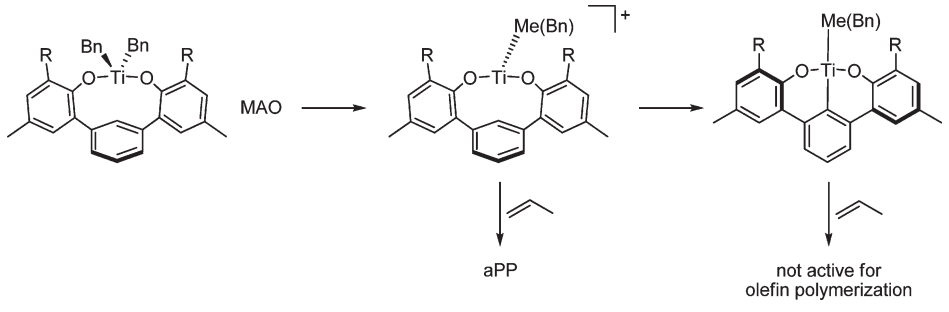

Protection of 2-*tert*-Butyl-4-methyl-5-bromophenol. Sodium hydride (2.7 g, 112.2 mmol) was suspended in anhydrous THF (25 mL). 2-*tert*-Butyl-4-methyl-5-bromophenol (22.73 g, 93.4 mmol) was dissolved in anhydrous THF (200 mL) and transferred by cannula onto the sodium hydride suspension. The mixture became magenta in color, and hydrogen gas was evolved. After 4 h, the mixture turned dark blue in color, and chloromethyl methyl ether (7.8 mL, 102.8 mmol) was syringed into the reaction flask. The mixture was stirred for 14 h. The mixture was quenched with water, concentrated, extracted in diethyl ether, washed with water (50 mL, 3×), dried over $MgSO_4$, filtered, and dried with a rotary evaporator to give a brownish-red oil: 25.1 g, 94%. ^{1}H NMR (500 MHz, $CDCl_3$): δ 1.42 (s, 9H, $C(CH_3)_3$), 2.28 (s, 3H, CH_3), 3.69 (s, 3H, CH_2OCH_3), 5.21 (s, 2H, CH_2OCH_3), 7.09 (s, 1H, C_6H_2), 7.25 (s, 1H, C_6H_2). ^{13}C NMR (125 MHz, $CDCl_3$): δ 20.71, 30.79, 35.56, 57.73, 99.32, 117.58, 127.58, 132.07, 134.39, 144.92, 150.66. HRMS (FAB+) obsd (M + H)$-H_2$ 285.0502; calcd for $C_{13}H_{18}BrO_2$, 285.0490.

Genceral Procedure for the Ligand Coupling Reaction. The protected bromophenol (3.3 mmol) was dissolved in THF (30 mL) in a glass vessel with a Köntes valve and cooled to just above its freezing point (−100 °C). *tert*-Butyl lithium (6.6 mmol) was added dropwise, and the reaction was stirred for 30 min to give a cloudy, light brown mixture. Zinc chloride (2.2 mmol) was added to the reaction mixture and stirred for 30 min to give a transparent orange solution. The dibromo-linker (1.5 mmol) and tetrakis(triphenylphosphine)palladium (0.03 mmol) were added to the reaction mixture which was sealed and placed in an oil bath. The mixture was heated at 70 °C overnight. The reaction was quenched with H_2O and concentrated under reduced pressure. The remaining aqueous sludge was extracted in diethyl ether or CH_2Cl_2, dried over $MgSO_4$, filtered, and dried with a rotary evaporator. The crude product was suspended in acidified methanol and heated to reflux to remove both impurities and the protecting group. After cooling to room temperature, filtration or removal of volatiles with a rotary evaporator of the neutralized suspension gave the desired product. If necessary, further purification was achieved by column chromatography (9:1, hexanes:CH_2Cl_2) or Kugelröhr distillation.

1-H$_2$. Pale yellow solid: 507 mg, 60%. ^{1}H NMR (500 MHz, $CDCl_3$): δ 1.79 (s, 12H, Ad), 2.09 (s, 6H, Ad), 2.23 (s, 12H, Ad), 2.37 (s, 6H, CH_3), 7.15 (s, 2H, C_6H_2), 7.29 (s, 2H, C_6H_2) 7.62 (d, 2H, *m*-C_5H_3N, J = 8 Hz), 7.96 (t, 1H, *p*-C_5H_3N, J = 8 Hz), 10.51 (bs, 2H, O*H*). ^{13}C NMR (125 MHz, $CDCl_3$): δ 21.22, 29.37, 37.39, 40.57, 120.55, 121.99, 126.47, 128.31, 129.89, 138.25, 139.94, 153.56, 157.25. HRMS (FAB+) obsd (M + H)$-H_2$ 558.3345; calcd for $C_{39}H_{44}NO_2$, 558.3372.

2-H$_2$. Pale yellow solid: 730 mg, 42%. ^{1}H NMR (500 MHz, $CDCl_3$): δ 1.49 (s, 18H, $C(CH_3)_3$), 2.39 (s, 6H, CH_3), 7.23 (s, 2H, C_6H_2), 7.33 (s, 2H, C_6H_2) 7.64 (d, 2H, *m*-C_5H_3N, J = 8 Hz), 7.97 (t, 1H, *p*-C_5H_3N, J = 8 Hz), 10.58 (s, 2H, O*H*). ^{13}C NMR (125 MHz, $CDCl_3$): δ 21.19, 29.75, 35.26, 120.48, 121.81, 126.64, 128.16, 129.95, 138.03, 139.95, 153.42, 157.24. HRMS (FAB+) obsd M+ 403.2507; calcd for $C_{27}H_{33}NO_2$, 403.2511.

3-H$_2$. Beige solid: 13.2 g, 36%. ^{1}H NMR (500 MHz, $CDCl_3$): δ 1.79 (s, 12H, Ad), 2.09 (s, 6H, Ad), 2.18 (s, 12H, Ad), 2.33 (s, 6H, CH_3), 5.29 (s, 2H, O*H*), 6.94 (s, 2H, C_6H_2), 7.07 (s, 2H, C_6H_2), 7.49 (d, 2H, *m*-C_6H_4, J = 7.5 Hz), 7.58 (s, 1H, C_6H_4), 7.59 (t, 1H, *p*-C_6H_4, J = 7.5 Hz). ^{13}C NMR (125 MHz, $CDCl_3$): δ 21.05, 29.31, 37.21, 40.73, 127.72, 128.29, 129.04, 129.31, 130.41, 131.05, 136.69, 139.10, 149.05. HRMS (FAB+) obsd M+ 558.3486; calcd for $C_{40}H_{46}O_2$, 558.3498.

4-H$_2$. Pale yellow crystalline solid: 1.9 g, 67%. ^{1}H NMR (500 MHz, $CDCl_3$): δ 1.47 (s, 18H, $C(CH_3)_3$), 2.35 (s, 6H, CH_3), 5.33 (s, 2H, O*H*), 6.97 (s, 2H, C_6H_2), 7.15 (s, 2H, C_6H_2), 7.52 (d, 2H, *m*-C_6H_4, J = 7.5 Hz), 7.58 (s, 1H, C_6H_4), 7.63 (t, 1H, *p*-C_6H_4, J = 7.5 Hz). ^{13}C NMR (125 MHz, $CDCl_3$): δ 21.02, 29.91, 35.08, 127.82, 128.26, 128.53, 129.00, 129.19, 130.47, 130.96, 136.45, 139.12, 148.91. HRMS (FAB+) obsd M+ 402.2555; calcd for $C_{28}H_{34}O_2$, 402.2559.

Synthesis of 1-TiCl$_2$(THF). Potassium benzyl (47 mg, 0.357 mmol) and **1-H$_2$** (100 mg, 0.178 mmol) were dissolved in THF (15 mL) and stirred for 30 min. This solution was added to $TiCl_4(THF)_2$ (60 mg, 0.178 mmol) and allowed to stir for 30 min. The THF was removed *in vacuo*. The resulting solid was suspended in diethyl ether and filtered. The filtrate was dried under vacuum to give a dark red crystalline solid: 77 mg, 58%. ^{1}H NMR (300 MHz, C_6D_6): δ 0.81 (m, 4H, THF), 2.01 (dd, 18H, Ad), 2.25 (s, 6H, CH_3), 2.61 (s, 12H, Ad), 3.39 (m, 4H, THF), 6.89 (d, 2H, *m*-C_5H_3N), 7.00 (t, 1H, *p*-C_5H_3N), 7.16 (s, 2H, C_6H_2), 7.28 (s, 2H, C_6H_2). Analysis: Calculated (Found) C: 69.05 (68.44); H: 6.74 (7.14); N: 1.87 (1.93); Ti: 6.40 (5.94).

Synthesis of 1-Ti(O^{i}Pr)$_2$. Titanium tetraisopropoxide (100 mg, 0.35 mmol) was dissolved in benzene (10 mL). **1-H$_2$** (200 mg, 0.35 mmol) predissolved in benzene (10 mL) was added to the titanium. The reaction was heated overnight at 80 °C. After cooling, the solvent was removed *in vacuo* to give a yellow solid: 142 mg, 56%. ^{1}H NMR (300 MHz, C_6D_6): δ 1.10 (s, 12H, $CH(CH_3)_2$), 1.95 (dd, 12H, Ad), 2.23 (s, 6H, Ad), 2.35 (s, 6H, CH_3), 2.56 (s, 12H, Ad), 5.04 (m, 2H, $CH(CH_3)_2$), 7.00 (t, 1H, *p*-C_5H_3N), 7.10 (d, 2H, *m*-C_5H_3N), 7.21 (s, 2H, C_6H_2), 7.35 (s, 2H, C_6H_2).

Synthesis of 1-VCl(THF)$_2$. Potassium benzyl (93 mg, 0.714 mmol) and **1-H$_2$** (200 mg, 0.357 mmol) were dissolved in THF (15 mL) and stirred for 30 min. This solution was added to $VCl_3(THF)_3$ (133 mg, 0.357 mmol) and allowed to stir for 30 min. The THF was removed *in vacuo*. The resulting solid was suspended in diethyl ether and filtered. The filtrate was dried under vacuum to give an orange/brown solid: 166 mg, 59%. ^{1}H NMR (C_6D_6): paramagnetic. Magnetic moment: μ_{eff} = 2.90(2) μ_B. Analysis: Calculated (Found) C: 71.37 (72.04); H: 6.92 (7.53); N: 1.85 (1.70); Cl: 4.68 (4.6).

General Procedure for the Synthesis of Dibenzyl Complexes. The tetrabenzyl complex of titanium, zirconium, or hafnium (0.357 mmol) was dissolved in toluene, pentane, petroleum ether, or diethyl ether (10 mL). The ligand (0.357 mmol) predissolved in the same solvent (10 mL) was added to the metal. The reaction was stirred for 1 h. The solvent was removed *in vacuo*. Recrystallization was achieved by dissolving in pentane or petroleum ether and cooling to −35 °C for a few days.

1-TiBn$_2$. Orange solid: 136 mg, 71%. ^{1}H NMR (300 MHz, C_6D_6): δ 1.88 (dd, 12H, Ad), 2.25 (s, 6H, Ad), 2.33 (s, 6H, CH_3), 2.87 (s, 12H, Ad), 4.05 (s, 4H, CH_2), 6.30 (t, 2H, C_6H_5), 6.47 (t, 4H, C_6H_5), 6.71 (t, 1H, *p*-C_5H_3N), 6.87 (m; 2H, *m*-C_5H_3N; 4H, C_6H_5; 2H, C_6H_2), 7.38 (s, 2H, C_6H_2). Analysis: Calculated (Found) C: 80.79 (80.57); H: 7.29 (7.18); N: 1.78 (1.76).

2-TiBn$_2$. Orange solid: 137 mg, 86%. ^{1}H NMR (500 MHz, C_6D_6): δ 2.27 (s, 18H, $C(CH_3)_3$), 2.57 (s, 6H, CH_3), 4.13 (s, 4H, CH_2), 6.59 (t, 2H, C_6H_5, J = 7 Hz), 6.76 (t, 4H, C_6H_5, J = 8 Hz), 6.99 (t, 1H, *p*-C_5H_3N, J = 8 Hz), 6.80 (d, 4H, C_6H_5, J = 7.5 Hz), 7.14 (s, 2H, C_6H_2), 7.42 (s 2H, C_6H_2), 7.73 (d, 2H, *m*-C_5H_3N, J = 2 Hz). ^{13}C NMR (125 MHz, C_6D_6): δ 21.65, 31.68, 36.00, 85.53, 123.15, 123.68, 129.72, 129.93, 130.84, 137.02, 137.76, 139.02, 156.96, 157.11.

3-TiBn$_2$. Berry red solid: 131 mg, 69%. ^{1}H NMR (300 MHz, C_6D_6): δ 1.84 (dd, 12H, Ad), 2.20 (s, 6H, Ad), 2.27 (s, 6H, CH_3), 2.80 (s, 12H, Ad), 3.71 (s, 2H, CH_2), 4.19 (s, 2H, CH_2), 6.44 (t, 1H, *p*-C_6H_4), 6.56 (d, 2H, *m*-C_6H_4), 6.62 (s, 1H, C_6H_4), 6.65 (d, 2H, C_6H_5), 6.67 (d, 2H, C_6H_5), 6.86 (s, 2H, C_6H_2), 6.94 (t, 4H, C_6H_5), 7.28 (s, 2H, C_6H_2), 7.38 (d, 2H, C_6H_5).

4-TiBn$_2$. Dark red crystals: 219 mg, 55%. ^{1}H NMR (500 MHz, C_6D_6): δ 1.65 (s, 18H, $C(CH_3)_3$), 2.02 (s, 2H, CH_2), 2.26 (s, 6H, CH_3), 3.49 (s, 2H, CH_2), 6.65 (s, 1H, C_6H_4), 6.67 (d, 2H, J = 7 Hz, C_6H_5), 6.75 (t, 1H, J = 7.5 Hz, C_6H_5), 6.90 (m, 3H, J = 7.5 Hz, C_6H_5), 7.03 (d, 2H, J = 8 Hz, C_6H_5), 7.06 (bs, 2H, C_6H_2), 7.10 (m, 5H, J = 8.5 Hz, C_6H_4 and C_6H_5), 7.28 (d, 2H, J = 2 Hz, C_6H_2). ^{13}C NMR (125 MHz, C_6D_6): δ 21.54, 30.72, 35.92, 94.85, 96.99, 124.14, 124.34, 127.22, 127.92, 128.01, 128.09, 128.14,

128.29, 128.84, 128.91, 131.84, 131.99, 135.84, 138.28, 142.30, 145.06, 146.41, 161.75.

1-ZrBn$_2$. Yellow solid: 147 mg, 99%. ^{1}H NMR (500 MHz, C_6D_6): δ 1.92 (dd, 12H, Ad, J = 12 Hz, J = 60 Hz), 2.22 (s, 6H, Ad), 2.28 (s, 6H, CH_3), 2.62 (s, 12H, Ad), 3.42 (s, 4H, CH_2), 6.27 (t, 2H, C_6H_5, J = 7.5 Hz), 6.46 (t, 4H, C_6H_5, J = 8 Hz), 6.71 (s, 2H, C_6H_2), 6.81 (t, 1H, p-C_5H_3N, J = 8.5 Hz), 6.87 (d, 2H, m-C_5H_3N, J = 7.5 Hz), 6.98 (d, 4H, C_6H_5, J = 7 Hz), 7.25 (s, 2H, C_6H_2). ^{13}C NMR (125 MHz, C_6D_6): δ 21.61, 30.07, 38.01, 42.29, 63.04, 122.91, 125.16, 126.03, 129.13, 129.39, 129.67, 130.11, 130.40, 130.56, 137.72, 138.59, 154.81, 159.75.

1-HfBn$_2$. Tan solid: 81 mg, 98%. ^{1}H NMR (500 MHz, C_6D_6): δ 1.92 (dd, 12H, Ad, J = 12 Hz, J = 62 Hz), 2.22 (s, 6H, Ad), 2.29 (s, 6H, CH_3), 2.65 (s, 12H, Ad), 3.16 (s, 4H, CH_2), 6.32 (t, 2H, C_6H_5, J = 7 Hz), 6.49 (t, 4H, C_6H_5, J = 8 Hz), 6.70 (s, 2H, C_6H_2), 6.74 (t, 1H, p-C_5H_3N, J = 8 Hz), 6.84 (d, 2H, m-C_5H_3N, J = 8 Hz), 6.98 (d, 4H, C_6H_5, J = 11 Hz), 7.28 (s, 2H, C_6H_2). ^{13}C NMR (125 MHz, C_6D_6): δ 21.59, 30.08, 38.04, 42.22, 69.81, 123.06, 124.96, 126.03, 128.89, 129.049, 129.67, 130.02, 130.28, 130.67, 138.27, 138.89, 155.34, 159.44.

Propylene Polymerization. An Andrews Glass Co. vessel was charged with MAO and toluene and fitted with a pressure regulator with a Swagelok quick-connect valve and septum. The vessel was cooled to 0 °C, and propylene was condensed (30 mL). The catalyst was dissolved in toluene and injected into the vessel. After the polymerization was complete, the system was vented and the residue was quenched with acidified methanol. The polymers were filtered and dried under vacuum prior to analysis.

Fractionation. A Kumagawa extractor was used for the fractionation experiment. Each solvent (diethyl ether, hexanes, and heptanes) was refluxed for 36 h. The solvent was transferred to a round-bottom flask and dried with a rotary evaporator. The polymers were dried on the high-vacuum line prior to analysis.

Ethylene/1-Octene Polymerization. Specially made 15 mL Schlenk flasks that fit septa on the side arm were charged with MAO (1000 equiv) and 1-octene. Toluene was vacuum transferred into the reaction vessels in the desired amount after degassing the 1-octene. An atmosphere of ethylene was introduced after the reaction vessel warmed to room temperature. A catalyst solution in toluene was injected through the side arm while ethylene was flowing. The reaction vessels were left open to the ethylene source such that a constant atmosphere of ethylene was always present. The polymerizations were quenched with acidified methanol. The polymers were filtered and dried under vacuum prior to analysis.

Polymer ^{13}C NMR Analysis. All samples were dissolved in 10 mm NMR tubes in a mixture of solvent (tetrachloroethane-d_2/o-dichlorobenzene-d_4 (1/4 v/v)) with typical concentrations of 0.1 g/mL. The tubes were then heated in a heating block set at 150 °C. The sample tubes were repeatedly vortexed and heated to achieve a homogeneous flowing fluid. Finally, the sample tubes were left in the heat block for 12 h. The ^{13}C NMR spectra were taken on a Varian Inova Unity 400 MHz spectrometer. The following acquisition parameters were used: 1.4 s relaxation delay, 2.6 s acquisition time, 90° pulse of 14.5 μs, full NOE with Waltz decoupling, 2000−8000 scans. All measurements were taken without sample spinning and at 126 ± 1 °C, calibrated by ethylene glycol. The ^{13}C NMR spectra were referenced at 74.24 ppm for the center peak of tetrachloroethane-d_2.

Acknowledgment. This work has been supported by the USDOE Office of Basic Energy Sciences (Grant DE-FG03-85ER13431). The authors thank Lawrence M. Henling and Michael W. Day of Caltech for mounting and solving the crystal structures. We also acknowledge Dr. Sara B. Klamo of The Dow Chemical Company for assistance with polymer characterization. The Bruker KAPPA APEXII X-ray diffractometer was purchased via an NSF CRIF:MU award to the California Institute of Technology, CHE-0639094.

Supporting Information Available: Additional tables, figures, and all CIFs. This material is available free of charge via the Internet at http://pubs.acs.org.

References and Notes

(1) *Chem. Eng. News* **1998**, *76*, 1.
(2) Brintzinger, H. H.; Fischer, D.; Mulhaupt, R.; Rieger, B.; Waymouth, R. M. *Angew. Chem., Int. Ed. Engl.* **1995**, *34*, 1143–1170.
(3) Britovsek, G. J. P.; Gibson, V. C.; Wass, D. F. *Angew. Chem., Int. Ed.* **1999**, *38*, 428–447.
(4) Coates, G. W. *Chem. Rev.* **2000**, *100*, 1223–1252.
(5) Coates, G. W.; Hustad, P. D.; Reinartz, S. *Angew. Chem., Int. Ed.* **2002**, *41*, 2236–2257.
(6) Gibson, V. C.; Spitzmesser, S. K. *Chem. Rev.* **2003**, *103*, 283–315.
(7) Resconi, L.; Cavallo, L.; Fait, A.; Piemontesi, F. *Chem. Rev.* **2000**, *100*, 1253–1345.
(8) Agapie, T.; Henling, L. M.; DiPasquale, A. G.; Rheingold, A. L.; Bercaw, J. E. *Organometallics* **2008**, *27*, 6245–6256.
(9) Chan, M. C. W.; Kui, S. C. F.; Cole, J. M.; McIntyre, G. J.; Matsui, S.; Zhu, N.; Tam, K.-H. *Chem.—Eur. J.* **2006**, *12*, 2607–2619.
(10) Chan, M. C. W.; Tam, K.-H.; Pui, Y.-L.; Zhu, N. *J. Chem. Soc., Dalton Trans.* **2002**, 3085–3087.
(11) Chan, M. C. W.; Tam, K.-H.; Zhu, N.; Chiu, P.; Matsui, S. *Organometallics* **2006**, *25*, 785–792.
(12) Tam, K.-H.; Lo, J. C. Y.; Guo, Z.; Chan, M. C. W. *J. Organomet. Chem.* **2007**, *692*, 4750–4759.
(13) Gademann, K.; Chavez, D. E.; Jacobsen, E. N. *Angew. Chem., Int. Ed.* **2002**, *41*, 3059–3061.
(14) Milne, J. E.; Buchwald, S. L. *J. Am. Chem. Soc.* **2004**, *126*, 13028–13032.
(15) Evans, D. F. *J. Chem. Soc.* **1959**, 2003–2005.
(16) Agapie, T.; Day, M. W.; Bercaw, J. E. *Organometallics* **2008**, *27*, 6123–6142.
(17) Tonks, I. A.; Henling, L. M.; Day, M. W.; Bercaw, J. E. *Inorg. Chem.* **2009**, *48*, 5096–5105.
(18) The catalysts appeared to be active for at least 2 h, although all polymerizations reported here were quenched after 30 min.
(19) Frank, H. *Oster. Chem. Zeit.* **1967**, *68*, 360–361.
(20) Zambelli, A.; Sessa, I.; Grisi, F.; Fusco, R.; Accomazzi, P. *Macromol. Rapid Commun.* **2001**, *22*, 297–310.
(21) Gambarotta, S. *Coord. Chem. Rev.* **2003**, *237*, 229–243.
(22) Schmidt, R.; Welch, M. B.; Knudsen, R. D.; Gottfried, S.; Alt, H. G. *J. Mol. Catal. A: Chem.* **2004**, *222*, 17–25.
(23) Sato, Y.; Nakayama, Y.; Yasuda, H. *J. Appl. Polym. Sci.* **2003**, *89*, 1659–1662.
(24) Doi, Y.; Suzuki, S.; Soga, K. *Macromolecules* **1986**, *19*, 2896–2900.
(25) Groysman, S.; Tshuva, E. Y.; Reshef, D.; Gendler, S.; Goldberg, I.; Kol, M.; Goldschmidt, Z.; Shuster, M.; Lidor, G. *Isr. J. Chem.* **2002**, *42*, 373–381.
(26) Lin, S.; Waymouth, R. M. *Macromolecules* **1999**, *32*, 8283–8290.
(27) De Rosa, C.; Auriemma, F.; Spera, C.; Talarico, G.; Tarallo, O. *Macromolecules* **2004**, *37*, 1441–1454.
(28) Bovey, F. A.; Tiers, G. V. D. *J. Polym. Sci.* **1960**, *44*, 173–182.
(29) Doi, Y.; Asakura, T. *Makromol. Chem.* **1975**, *176*, 507–509.
(30) Doi, Y.; Suzuki, E.; Keii, T. *Makromol. Chem., Rapid Commun.* **1981**, *2*, 293–297.
(31) Sheldon, R. A.; Rueno, T.; Tsunetsugu, T.; Furakawa, J. *J. Polym. Sci.* **1965**, *3*, 23–26.
(32) Similar results were expected for 1-TiCl$_2$(THF), 1-TiBn$_2$, 2-TiBn$_2$, and 1-ZrBn$_2$ because the ^{13}C NMR spectra for crude polymer are comparable, implying that the coordinated THF does not influence the type of polymer produced.
(33) Golisz, S. R.; Bercaw, J. E. Manuscript in preparation.
(34) Trimethylaluminum was added to the ligands 1-H$_2$ and 2-H$_2$ to form bisphenolate aluminum methyl complexes (1-AlMe and 2-AlMe). Both of these aluminum species were subjected to standard propylene polymerization conditions, and in neither case was any PP observed. Additional reactions where only ligand was subjected to standard propylene polymerization conditions were also performed in the hope that an aluminum species which was capable of polymerizing propylene might form in situ. Again, no polymer was observed.
(35) Makio, H.; Kashiwa, N.; Fujita, T. *Adv. Synth. Catal.* **2002**, *344*, 477–493.

(36) Mitani, M.; Saito, J.; Ishii, S.-I.; Nakayama, Y.; Makio, H.; Matsukawa, N.; Matsui, S.; Mohri, J.-I.; Furuyama, R.; Terao, H.; Bando, H.; Tanaka, H.; Fujita, T. *Chem. Rec.* **2004**, *4*, 137–158.
(37) Calderazzo, F.; Englert, U.; Pampaloni, G.; Santi, R.; Sommazzi, A.; Zinna, M. *J. Chem. Soc., Dalton Trans.* **2005**, 914–922.
(38) NMR scale reactions were performed using 1-H_2 or 1-$TiCl_2$(THF) in benzene-d_6 to show no reaction upon mixing at room temperature, nor was there a reaction at 90 °C.
(39) Randall, J. C. *J. Macromol. Sci., Rev. Macromol. Chem. Phys.* **1989**, *C29*, 201–317.
(40) Hagen, H.; Boersma, J.; Lutz, M.; Spek, A. L.; van Koten, G. *Eur. J. Inorg. Chem.* **2001**, 117–123.
(41) Wu, J.-Q.; Pan, L.; Li, Y.-G.; Liu, S.-R.; Li, Y.-S. *Organometallics* **2009**, *28*, 1817–1825.
(42) Burger, B. J.; Bercaw, J. E. *ACS Symp. Ser.* **1987**, *357*, 79–98.
(43) Marvich, R. H.; Brintzinger, H. H. *J. Am. Chem. Soc.* **1971**, *93*, 2046–2048.
(44) Manzer, L. *Inorg. Synth.* **1982**, *21*, 135–140.
(45) Zucchini, U.; Giannini, U.; Albizzat, E.; Dangelo, R. *J. Chem. Soc., Chem. Commun.* **1969**, 1174–1175.